Geologie en Mijnbouw **75:** 43–55, 1996.

Palinspastic reconstruction of Permo-Carboniferous basins involved in Alpine deformation: the Erill Castell–Estac basin, Southern Pyrenees, Spain

Carles Soriano[1], Joan Martí[1] & Josep-Maria Casas[2]

[1] *Institut de Ciències de la Terra 'Jaume Almera' (CSIC), Martí i Franquès s/n 08028 Barcelona, Spain;* [2] *Grup de Geodinàmica i analisi de conques, Departament de Geologia Dinàmica, Geofísica i Paleontologia, Facultat de Geologia, Universitat de Barcelona, Zona Universitària de Pedralbes, 08028 Barcelona, Spain*

Received 30 June 1994; accepted in revised form 26 March 1996

Key words: Alpine thrusts, Nogueres Zone, palinspastic restoration

Abstract

Permo-Carboniferous rocks are located in the lower thrust sheets of the Alpine antiformal stack in the Central Pyrenees. In order to study the geometry, distribution of facies, thickness and dynamics of Permo-Carboniferous basins, a detailed knowledge of Alpine tectonics is required, which has not always been taken into account by previous authors. This paper follows a different approach to the study of these basins. The Alpine structural units bounding the Permo-Carboniferous series of the eastern part of the Erill Castell–Estac basin have been mapped in detail, as a first step in this palinspastic restoration. This procedure has allowed: 1) to define some Alpine thrusts as inverted Permo-Carboniferous normal faults, 2) to constrain the age of several Permo-Carboniferous faults, 3) to differentiate the area studied as a volcano-tectonic depression, independent of the western part of the Erill Castell–Estac basin, and 4) to establish the paleogeographic position of the Permo-Carboniferous series and the minimum dimensions for the part of the basin studied.

Introduction

After the Variscan orogeny, Carboniferous and Permian continental sediments were deposited in the Southern Pyrenees. These sediments unconformably overlie previously deformed Variscan basement, and in turn are unconformably overlain by Lower Triassic. Occurrences of Permo-Carboniferous rocks are not continuous throughout the Pyrenees, as in some places Triassic beds rest directly on Variscan basement. The entire pre-Eocene series was deformed during the Alpine orogeny, and thus became incorporated in the Alpine structural units (Figures 1, 2).

One of the main features of the Permo-Carboniferous series in the Southern Pyrenees is the interlayering of thick volcanic beds with non-volcanic sediments. The volcanic rocks are of calc-alkaline orogenic type, predominantly rhyolitic and rhyodacitic pyroclastics. In the Southern Pyrenees, the volcanic activity was essentially continuous from the time of deposition of the Middle Stephanian (Upper Carboniferous) to the onset of Late Permian sedimentation, a duration of about 18 Ma (Martí 1986). Despite the considerable time period involved, no significant changes in the chemistry or facies of the Permo-Carboniferous volcanism have been observed (Martí 1986; Gilbert 1989).

Pyrenean Permo-Carboniferous rocks were first studied from a petrological and stratigraphic viewpoint by Dutch geologists (Mey et al. 1968; Nagtegaal 1969; Hartevelt 1970). Later studies focused on sedimentology and volcanology (Gisbert 1981, 1983; Bixel & Lucas 1983; Speksnijder 1985; Martí 1986; Martí & Mitjavila 1988; Gilbert & Rogers 1989; Besly & Collinson 1991). Detailed sedimentary and volcanic facies analysis of Permo-Carboniferous rocks allowed Martí (1986, 1991) to group these rocks of the Central and Eastern Pyrenees into four separate basins. From west to east these are: the Erill Castell–Estac, Cadí, Castellar de n'Hug and Campelles basins (see Martí 1991 for locations). The main features of these basins include the presence of calc-alkaline volcanism related

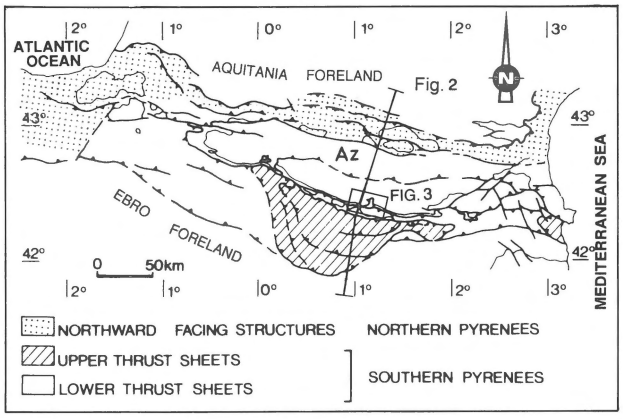

Figure 1. Structural sketch map of the Pyrenees, showing locations of Figures 2 and 3. The Lower Thrust Sheets are those involving Variscan basement, whereas the Upper Thrust Sheets only involve the Mesozoic and Tertiary cover, but no basement at all (Muñoz 1992). AZ = Axial Zone.

to the late stages of the Variscan orogeny, the presence of N–S-trending faults of Permo-Carboniferous age, and the narrow E–W-elongated arrangement of the Permo-Carboniferous outcrops in plan view (Figure 3). Following Soula et al. (1979), most authors have suggested a strike-slip control on the Permo-Carboniferous basin formation.

None of the previous studies took into account the effects of Alpine deformation, in particular the effects of the Alpine thrusting, on the structural units in which Permo-Carboniferous rocks occur today. This point is not relevant when stratigraphic sections are correlated within a structural unit, but is important when they are correlated between different units. Furthermore, it is difficult to establish the original basin dimensions if the direction and dimensions of younger thrust movements are not considered.

The aim of this contribution is to reconstruct the original dimensions and the facies distribution of one of the Permo-Carboniferous basins and to describe the significance of Permo-Carboniferous N–S-trending faults. To meet this objective we have studied the eastern part of the Erill Castell–Estac basin, which contains a well-exposed and complete volcanic sequence (Figure 3). As the rocks are deformed by a series of Alpine thrusts, a detailed knowledge of the Alpine structures becomes essential. Detailed mapping together with the construction of a series of balanced and restored geological cross-sections has allowed us to remove the effects of Alpine deformation, to establish the paleogeographic position of the Permo-Carboniferous series, to recognize E–W and N–S-trending Permo-Carboniferous normal faults (subsequently reactivated during Alpine deformation) and, finally, to determine the original dimensions of the basin.

Permo-Carboniferous stratigraphy of the Southern Pyrenees

The stratigraphy of the Permo-Carboniferous in the Southern Pyrenees has been established in detail by Gisbert (1981, 1983). Integrating lithological, sedimentological and structural data, this author divides the Permo-Carboniferous sequence into four units (Figure 4):

1 The Grey Unit, Middle Stephanian (Broutin & Gisbert 1985), which mainly comprises dacitic to rhyolitic pyroclastic deposits, andesitic lavas and, less commonly, rhyolitic lavas. Polygenetic sedimentary breccias and conglomerates are located near the base of this unit. They are known as the Aguiró Formation (Nagtegaal 1969). The thickness of the Grey Unit ranges between 60 and 1000 m.
2 The Transition Unit, Upper Stephanian–Lower Permian (Alvarez-Ramis 1985), overlies the Grey Unit, locally with a low-angle unconformity (Gisbert 1981, 1983; Besly & Collinson 1991), and consists of rhyodacitic ignimbrites and dacitic lavas, detrital deposits, coal beds and rare lacustrine limestone. The thickness of the Transition Unit varies from 80 m in the Erill Castell–Estac basin to 400 m in the Campelles basin, 100 km to the east, where it consists mainly of coals.
3 The Lower Red Unit, Lower Permian, rests conformably on the Transition Unit (Broutin & Gisbert 1985), and is mainly represented by fluvial deposits, but also contains massive rhyolitic lava flows and pyroclastic deposits. Its thickness ranges from 70 m in the Erill Castell–Estac basin to 300 m in the Castellar de n'Hug basin, 75 km to the east.
4 The Upper Red Unit, Upper Permian, overlies the Lower Red Unit with an angular unconformity and is entirely represented by fluvial deposits that are rich in volcanic fragments. The unit is absent in the Erill Castell–Estac basin and reaches a maximum thickness of 200 m in the Cadí basin, 50 km to the east.

The Bunter Sandstone Unit (Lower Triassic) unconformably overlies the Permo-Carboniferous and is composed entirely of fluvial sediments. The uncon-

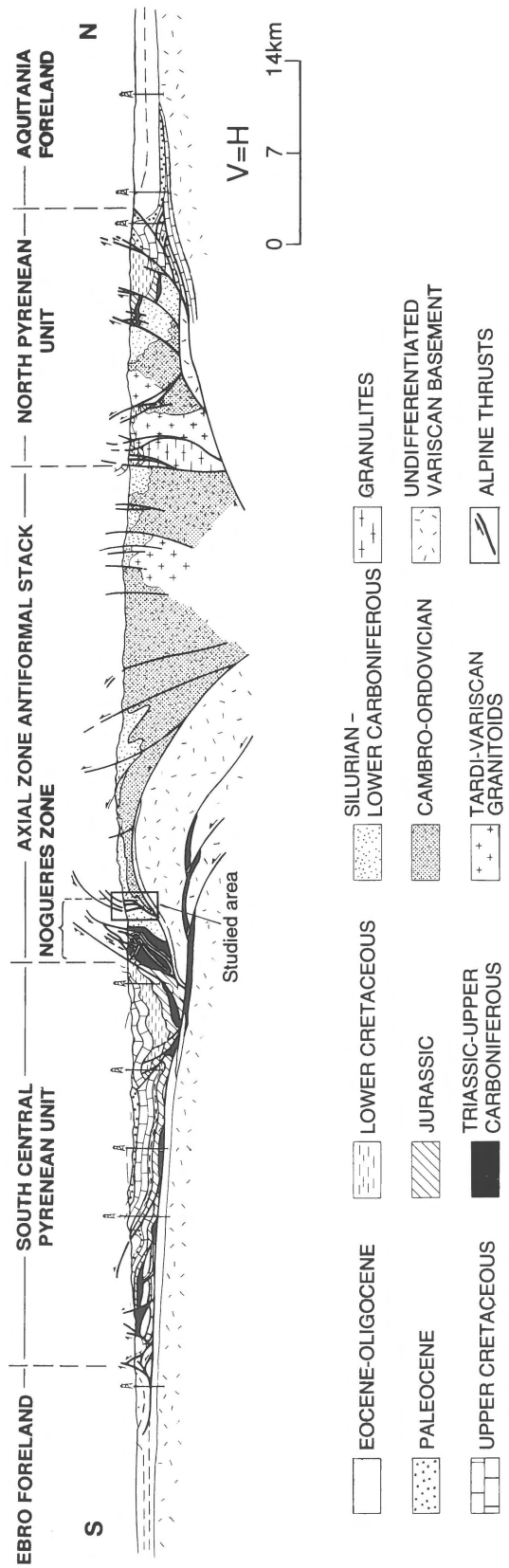

←

Figure 2. Cross-section through the Pyrenean orogenic belt, after Muñoz (1992).

formity surface is widely exposed and implies a hiatus of 37 Ma, where the Lower Triassic rests on the Lower Red Unit, and of 55 Ma, where the Lower Triassic rests directly on Variscan basement (Figure 4).

Permo-Carboniferous stratigraphy of the eastern part of the Erill Castell–Estac basin

The *Grey Unit* is the most widespread Permo-Carboniferous unit throughout the eastern part of the Erill Castell–Estac basin (Figure 5), where it is composed of a 50-m-thick sedimentary succession and overlying volcanic rocks. The sedimentary succession is known as the Aguiró Formation (Nagtegaal 1969), and is characterized by breccias and conglomerates which are interlayered with sandstones in the middle and upper parts of the succession. The pebbles are derived from Devonian limestones and Ordovician slates. The conglomerate beds commonly display scoured bases and imbricated pebbles, and have been interpreted as braided river deposits (Nagtegaal 1969). Volcanic rocks overlie the Aguiró Formation, but may also rest directly upon the Variscan basement. The thickness of the volcanic deposits is quite variable: e.g. about 1000 m to the east, and from 60 to 200 m to the west of the Estac village. Despite the variations in thickness, the volcanic facies of this package is quite similar to that in other parts of the eastern part of the Erill Castell–Estac basin. A detailed stratigraphic and facies analysis of the Estac volcanic succession, which is the most complete and best exposed in this basin, was presented by Martí (1986, 1991). In this succession the Grey Unit can be more than 1000 m thick, and is mainly composed of pyroclastic rocks (Figure 6). More than 15 ignimbrite units, interbedded with pyroclastic surge and fine ash-fall deposits as well as coal beds, can be distinguished.

The volcanic succession of the Grey Unit near Estac begins at its base with a thick unit of rhyolitic breccias which represent proximal deposits probably associated with dome explosions (Martí 1986). Above the rhyolitic breccias there are base surge deposits interbedded with ignimbrite units, and with coal beds representing brief non-eruptive periods. In these periods, shallow

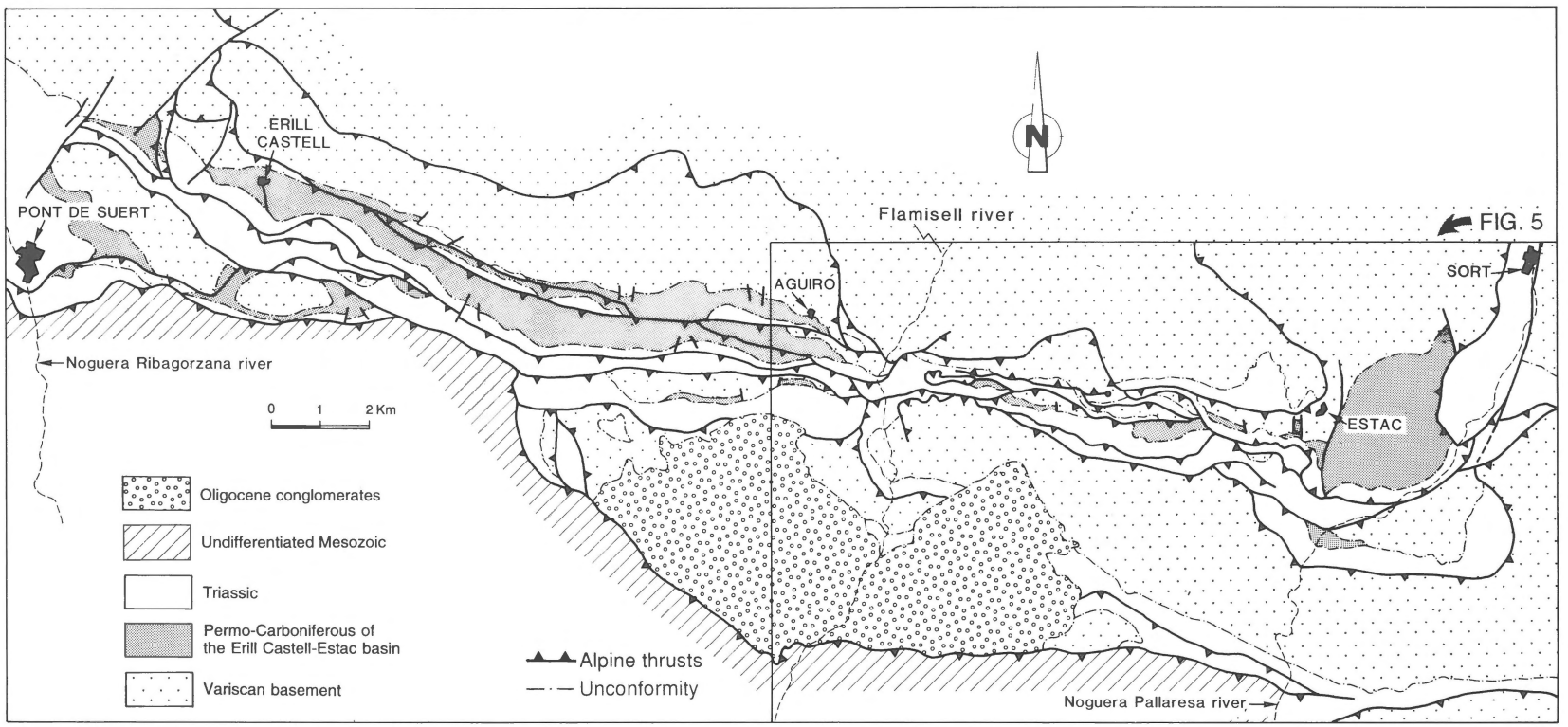

Figure 3. Geological map of the area between the Noguera Pallaresa and Noguera Ribagorzana rivers in the Southern Pyrenees, showing the location of the studied zone (Figure 5). Variscan basement, Permo-Carboniferous and Mesozoic were involved in Alpine deformation. Triassic includes: Lower Triassic sandstones, Middle Triassic limestones, and Upper Triassic evaporites that acted as an upper detachment level during Alpine deformation. Oligocene conglomerates are mainly post-orogenic.

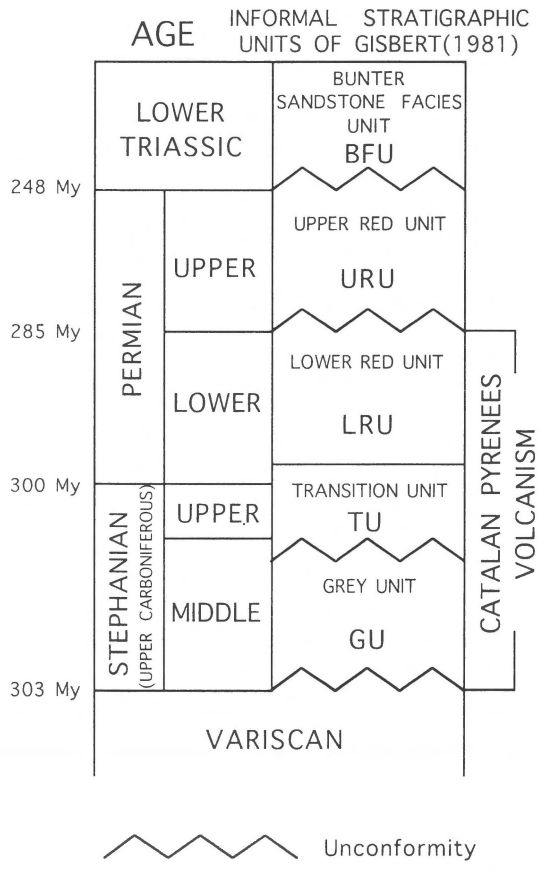

Figure 4. Ages of Permo-Carboniferous units in the Southern Pyrenees based on the Upper Carboniferous time scale of Hess & Lippolt (1986). The ages for the units are based on paleontological data from different authors (see text for references; drawing is not to scale).

lacustrine environments were established. The greater part of the Estac volcanics consist of a thick succession (> 1000 m) of ignimbrites and some horizons of pyroclastic surge and ash-fall deposits. The latter are always located on top of ignimbrite units and are interpreted as ash-cloud deposits accompanying pyroclastic flows (Martí 1986). No Plinian fallout deposits have been observed.

The Estac ignimbrite units have a rhyolitic to dacitic composition and are usually very thick (10 to 60 m). There is a notable absence of interbedded pumice fall deposits. The abundant rhyolite clasts in the ignimbrites suggest that eruptions formed domes or lava flows during the early volcanic episodes that preceded the pyroclastic flow eruptions. The presence of rhyolitic breccias at the base of the pyroclastic sequence is consistent with this interpretation.

In summary, the main characteristics of the pyroclastic sequence of Estac are as follows: 1) The sequence is several hundred metres thick, and no significant erosion surfaces separate the volcanic deposits. This suggests that rapid subsidence and active volcanism precluded significant sedimentation and erosion, especially for the middle and upper part of the sequence. 2) The lithological and sedimentological characteristics of the ignimbrites suggest that the ignimbrite-forming eruptions were not of Plinian type. A mechanism that involved large-scale continuous collapse of eruption columns may have produced many of these ignimbrites. 3) Sequences of similar characteristics have been described in recent volcanic areas associated with caldera-forming eruptions (Self 1983; Self et al. 1986). The eruptive mechanisms deduced to explain the origin of the Estac pyroclastics agree with a caldera-like mechanism. Hence these pyroclastics would represent intra-caldera facies. The characteristics exhibited by the Estac volcanics are similar to those of Grey Unit volcanics in other Permo-Carboniferous basins in the Southern Pyrenees (Martí 1991).

The *Transition Unit* is only exposed in the southeast of the studied area (Figure 5), where it directly overlies the Variscan basement and where it is overlain by Lower Triassic. The Transition Unit here is characterized by an 80-m-thick, upwards fining and thinning succession composed at its base of sandstone beds which have slightly scoured bases and which are interbedded with mudstones. Green and black mudstones with thin coal horizons appear in the middle section of the succession, and black limestones interbedded with shales near its top. Some thin lenses of volcanic ash can also be recognized. Sandstones of the unit's lower section display low-angle cross stratification and are interpreted as fluvial, whereas the rest of the unit is interpreted as lacustrine.

Lower Red Unit exposures are restricted to the east of the studied area. They are located southeast of Estac, overlying Grey Unit volcanics and overlain by Lower Triassic (Figure 5). The Lower Red Unit consists of a 70-m-thick red succession of conglomerate beds which have scoured bases and which are interlayered with sandstones and siltstones. The pebbles of the conglomerates are derived mostly from the Variscan basement, but also from volcanic rocks. Burrowing and iron reduction spots occur commonly in the sandstone and siltstone beds. Detailed stratigraphic and sedimentological analyses of this unit were presented by Nagtegaal (1969) for the western part of the Erill Castell–Estac basin, and by Gisbert (1981, 1983)

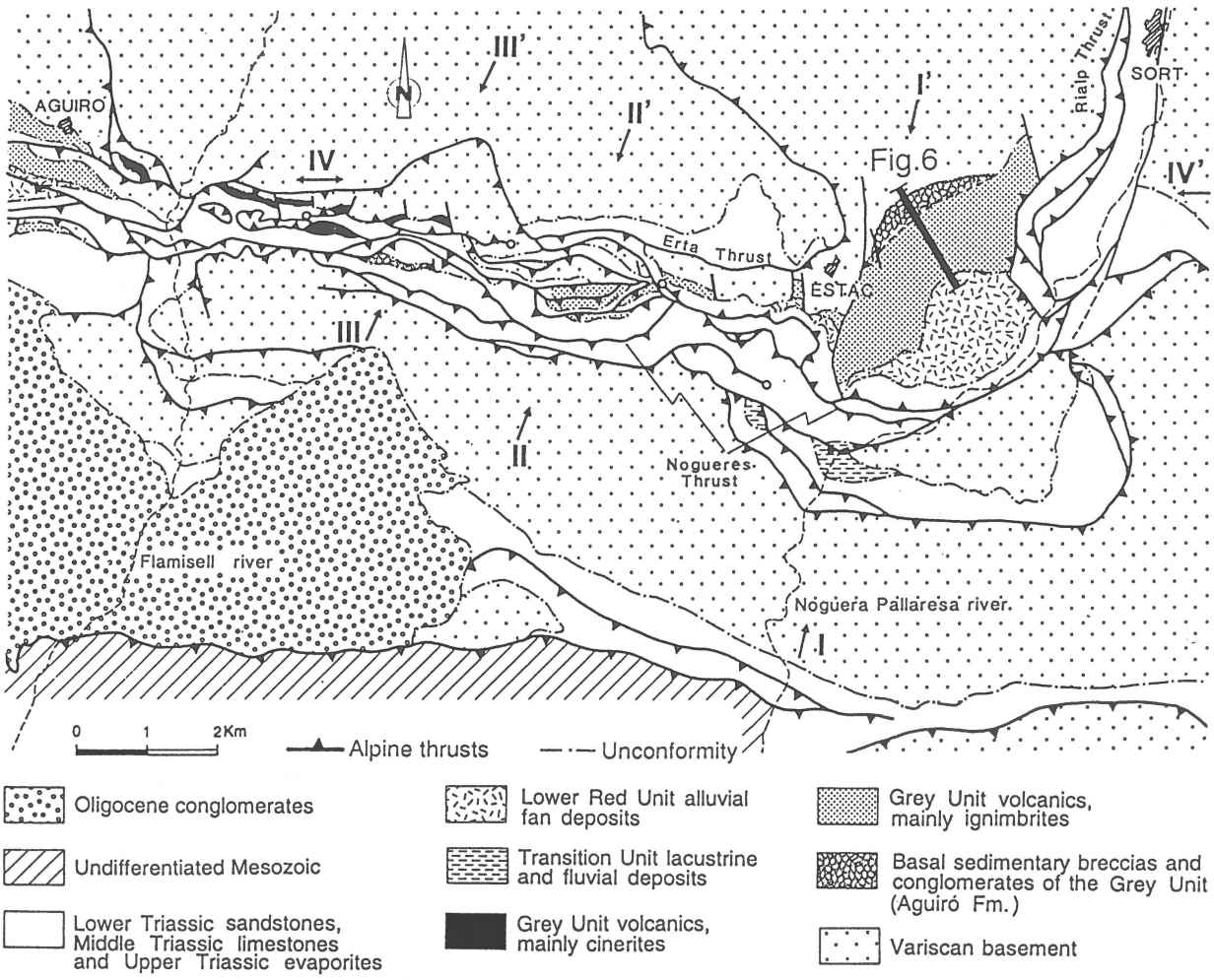

Figure 5. Geological map of the area between the Noguera Pallaresa and Flamisell rivers, including the eastern part of the Erill Castell–Estac Permo-Carboniferous basin, and showing locations of cross-sections in Figures 7 and 8, upon which palinspastic reconstruction is based, of stratigraphic column of Figure 6, and of longitudinal section IV-IV' of Figure 8.

and Speksnijder (1985) for the Cadí basin. All authors agree with the interpretation of the unit as alluvial fan sediments deposited in an arid climate.

Structural framework

As the Permo-Carboniferous rocks of the Pyrenees have been involved in Alpine deformation, a detailed knowledge of Alpine tectonics is required to reconstruct their original paleogeographic position.

The Pyrenees is an Alpine fold and thrust belt, trending WNW–ESE, that involves Variscan rocks of Cambrian to Early Carboniferous age, which are unconformably overlain by Late Carboniferous to Oligocene sediments (Figures 1, 2). The Pyrenean orogenic belt may be briefly described as: an imbricate thrust system that dips south in the north (the North Pyrenean Unit), an antiformal stack in the central part (the Axial Zone Antiformal Stack), and an imbricate thrust system dipping north in the south (the South Pyrenean Unit) (Muñoz 1992; Figures 1, 2). The Permo-Carboniferous is exposed only in the lower thrust sheets of the Axial Zone Antiformal Stack and has a narrow WNW–ESE shape in plan view, following the strike of the Alpine structural units (Figure 3).

Sheets forming the leading edge of the Axial Zone Antiformal Stack are known as the Nogueres Zone (Dalloni 1910). Nogueres thrust sheets were steepened, and even overturned, due to subsequent piggy-

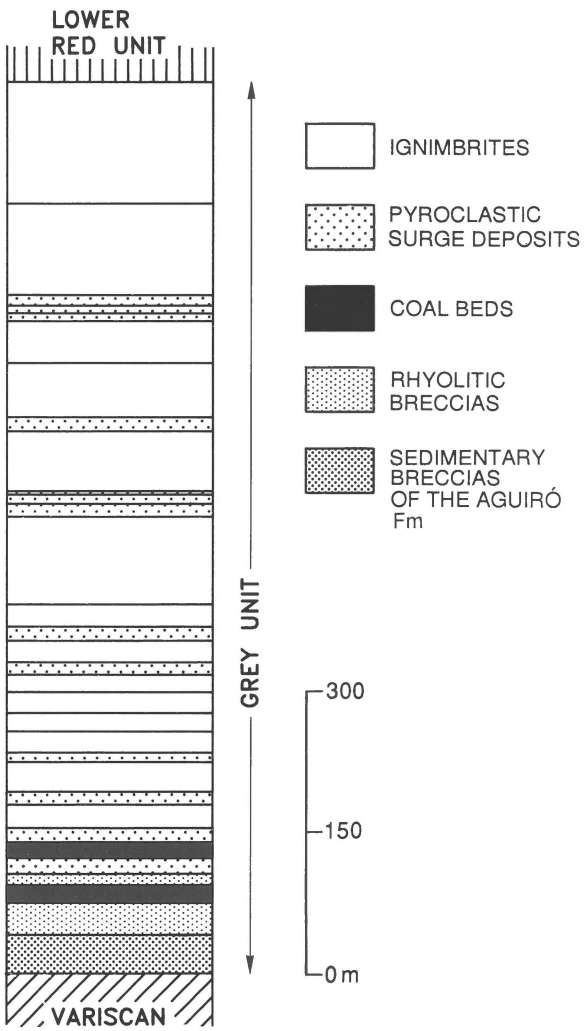

Figure 6. Simplified stratigraphic section of the Grey Unit (Martí 1991) east of the village of Estac. Horizontal lines within ignimbrites indicate different pyroclastic flows of the same eruptive process.

back emplacement of the lower thrust sheets (Muñoz 1992; Figures 2, 5, 7). In the studied area, the Alpine thrust sheets are composed of Variscan basement and of Permo-Carboniferous and Triassic rocks.

The lowest thrust of the Axial Zone Antiformal Stack cropping out in the studied area is called the Rialp thrust (Figure 5). It is gently domed (Figures 7, 8) and its hanging-wall is formed by Variscan basement and Permo-Carboniferous and Triassic rocks. The Permo-Carboniferous is incomplete. The Lower Red Unit lies unconformably on the Grey Unit, which in turn unconformably overlies the Variscan basement (Figures 5, 7). Triassic beds rest, again unconformably, on the Lower Red Unit. There are no Transition Unit rocks in the hanging-wall of the Rialp thrust. Erosion has allowed footwall exposure of the Rialp thrust as a tectonic window (Figures 5, 8). The footwall stratigraphy is restricted to Variscan basement and Triassic rocks, Permo-Carboniferous rocks being absent. The Lower Triassic unconformity is intersected in the hanging-wall of the Rialp thrust east of Estac, in the Pallaresa valley, forming the hanging-wall cutoff line (Figure 5), whereas the same unconformity is intersected in the footwall of the Rialp thrust north of Sort, outside the area mapped in Figure 5, forming the footwall cutoff line. Hence, displacement on the Rialp thrust is at least 4 km towards the SSW (Poblet 1991).

The Erta thrust unit is located on top of the Rialp thrust unit. The Erta thrust plane dips 50° to the south near the leading branch line with the Rialp thrust (Figure 7). The Erta thrust unit involves, in its hanging-wall, Variscan basement, Grey Unit volcanics, Lower Red Unit sediments, and Triassic rocks. There are no Permo-Carboniferous beds in the footwall, so Triassic beds lie directly on the Variscan basement. The Erta thrust trends approximately WNW–ESE, and departures from this mean direction are due to lateral ramps, for example:

a East of the village of Estac, where the Erta thrust trend changes from its mean direction towards NNW–SSE and the thrust cuts down into the footwall stratigraphic section (Figures 5, 8). The Estac volcanics of the Grey Unit in Figure 6 are located east of this lateral ramp, and the Lower Red Unit overlying the Grey Unit thickens eastwards (Figure 5).

b West of the Flamisell river, where the Erta thrust trend turns NNW–SSE and the thrust cuts down through the hanging-wall stratigraphic section (Figure 5). The Permo-Carboniferous succession of the western part of the Erill Castell–Estac basin is located west of this lateral ramp. The Lower Red Unit thickens westwards (Figures 5, 8). For the Rialp thrust, estimations of minimum displacement on the Erta thrust are possible because the same cutoff line (i.e. the frontal Lower Triassic cutoff line) crops out both in the hanging-wall and the footwall. Displacement on the Erta thrust is always to the SSW and decreases gradually westwards. In the vicinity of Estac it is about 2 km, whereas near the Noguera Ribagorzana river it has decreased to 500 m (Poblet 1991).

Stacked over the Erta thrust there are a variable number of minor thrust sheets with a duplex geometry (Figure 5). Thrusts bounding these sheets branch each other

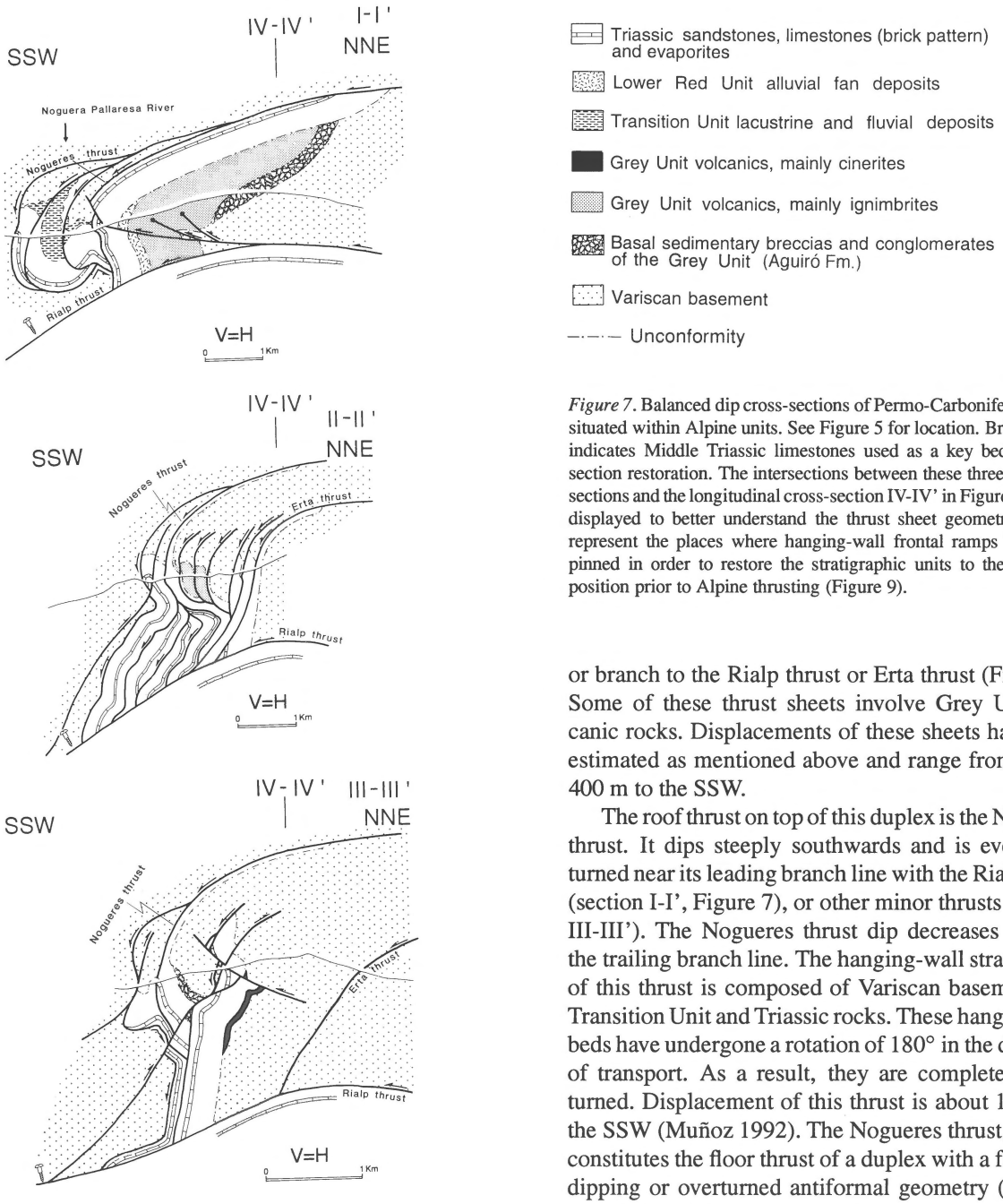

Figure 7. Balanced dip cross-sections of Permo-Carboniferous rocks situated within Alpine units. See Figure 5 for location. Brick pattern indicates Middle Triassic limestones used as a key bed in cross-section restoration. The intersections between these three dip cross-sections and the longitudinal cross-section IV-IV' in Figure 8 are also displayed to better understand the thrust sheet geometry. Screws represent the places where hanging-wall frontal ramps have been pinned in order to restore the stratigraphic units to their original position prior to Alpine thrusting (Figure 9).

or branch to the Rialp thrust or Erta thrust (Figure 7). Some of these thrust sheets involve Grey Unit volcanic rocks. Displacements of these sheets have been estimated as mentioned above and range from 100 to 400 m to the SSW.

The roof thrust on top of this duplex is the Nogueres thrust. It dips steeply southwards and is even overturned near its leading branch line with the Rialp thrust (section I-I', Figure 7), or other minor thrusts (section III-III'). The Nogueres thrust dip decreases towards the trailing branch line. The hanging-wall stratigraphy of this thrust is composed of Variscan basement, the Transition Unit and Triassic rocks. These hanging-wall beds have undergone a rotation of 180° in the direction of transport. As a result, they are completely overturned. Displacement of this thrust is about 11 km to the SSW (Muñoz 1992). The Nogueres thrust, in turn, constitutes the floor thrust of a duplex with a foreland-dipping or overturned antiformal geometry (sections I-I', II-II', Figure 7).

Thrust propagation in the Nogueres Zone was in piggy-back mode. As a consequence, the upper, southernmost sheets were steepened and overturned during emplacement of the lower, northernmost sheets. The regional thrust transport direction in the Nogueres Zone was obtained from the study of the orientation of fold axes and frontal cutoff lines with respect to the thrust-plane orientation. The Nogueres Zone thrust sheets

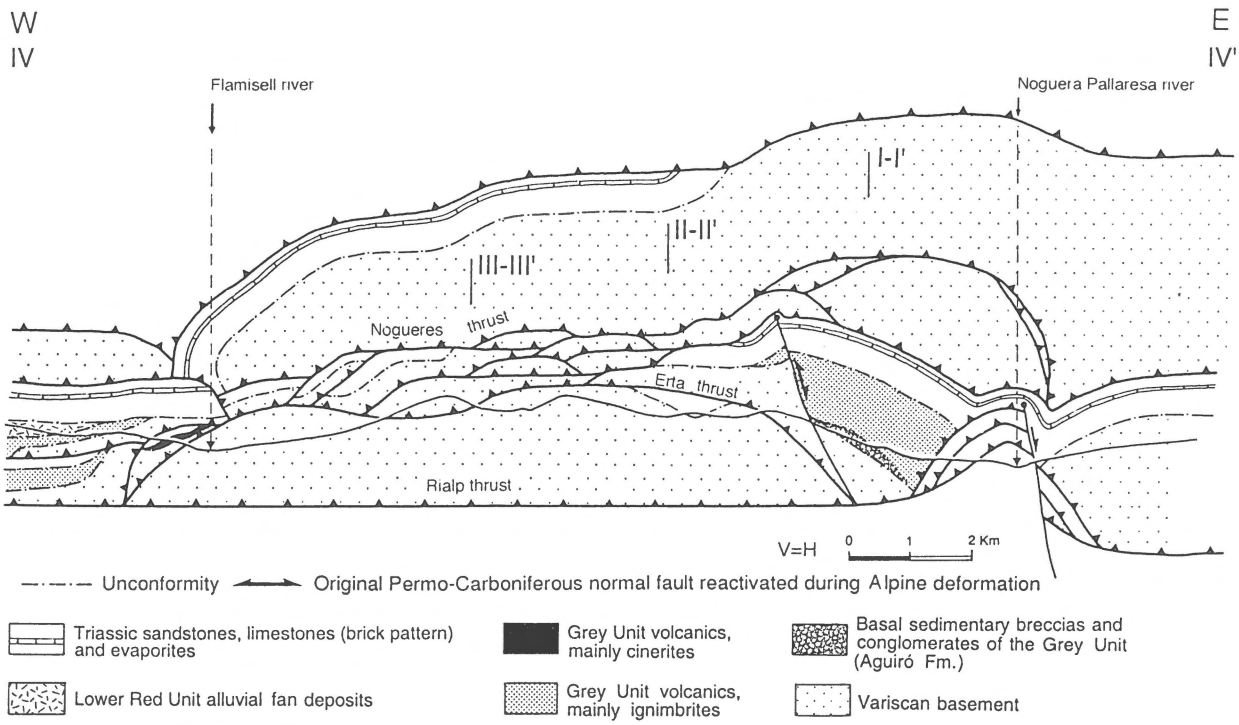

Figure 8. Longitudinal cross-section (normal to the thrust transport direction) of the Alpine units involving Permo-Carboniferous rocks. See Figure 5 for location. The part of the section above the topographic surface has been projected from the cross-sections in Figure 7 and from the map in Figure 5. Thrust emplacement is towards the reader.

have been displaced towards the SSW over a distance of 7 km (Muñoz 1992).

During the stacking of the Nogueres Zone, additional structures were generated. Firstly, north-directed, steeply southward-dipping backthrusts (sections II-II', III-III', Figure 7). Secondly, south-directed gently northward-dipping thrusts (sections I-I', III-III'). The strong dip of the backthrusts suggests that they were steepened during emplacement of the lower Nogueres Zone sheets. Thus their propagation took place prior to the eventual structuration of the Nogueres Zone.

Mapping of the Estac volcanics revealed the occurrence of Carboniferous to Permian near-vertical faults that are unconformably covered by the Lower Red Unit or the Triassic. These faults separate blocks with major differences in the thickness of the Permo-Carboniferous (Figures 5, 8). The faults strike between NNW–SSE and NNE–SSW. The strike displacements in plan view rarely exceed 200 m. Some of these faults have been reactivated during the Alpine orogeny as reverse or normal faults. An example is the N–S fault located east of the village of Estac. Its hanging wall (east block) is made up of 1000 m of volcanic and sedimentary rocks of the Grey Unit, whereas its footwall (west block) contains only 200 m of volcanic Grey Unit rocks (Figure 8). This difference in thickness, together with the interpretation of the Estac volcanics as intracaldera deposits (see above), allows us to consider this fault as one of the caldera walls. Movement on the fault in Permo-Carboniferous times was synchronous with the deposition of the Grey Unit volcanics. Later on normal faulting took place during the Alpine orogeny. Hence this fault cuts the Triassic unconformity and folds an earlier Alpine thrust (Figure 8).

Reconstruction of the eastern part of the Erill Castell–Estac basin

Palinspastic reconstruction for the eastern part of the Erill Castell-Estac basin was undertaken using three balanced and restored geological cross-sections (Figure 7, 9).

In Figure 10, all Permo-Carboniferous exposures of this eastern part have been palinspastically restored.

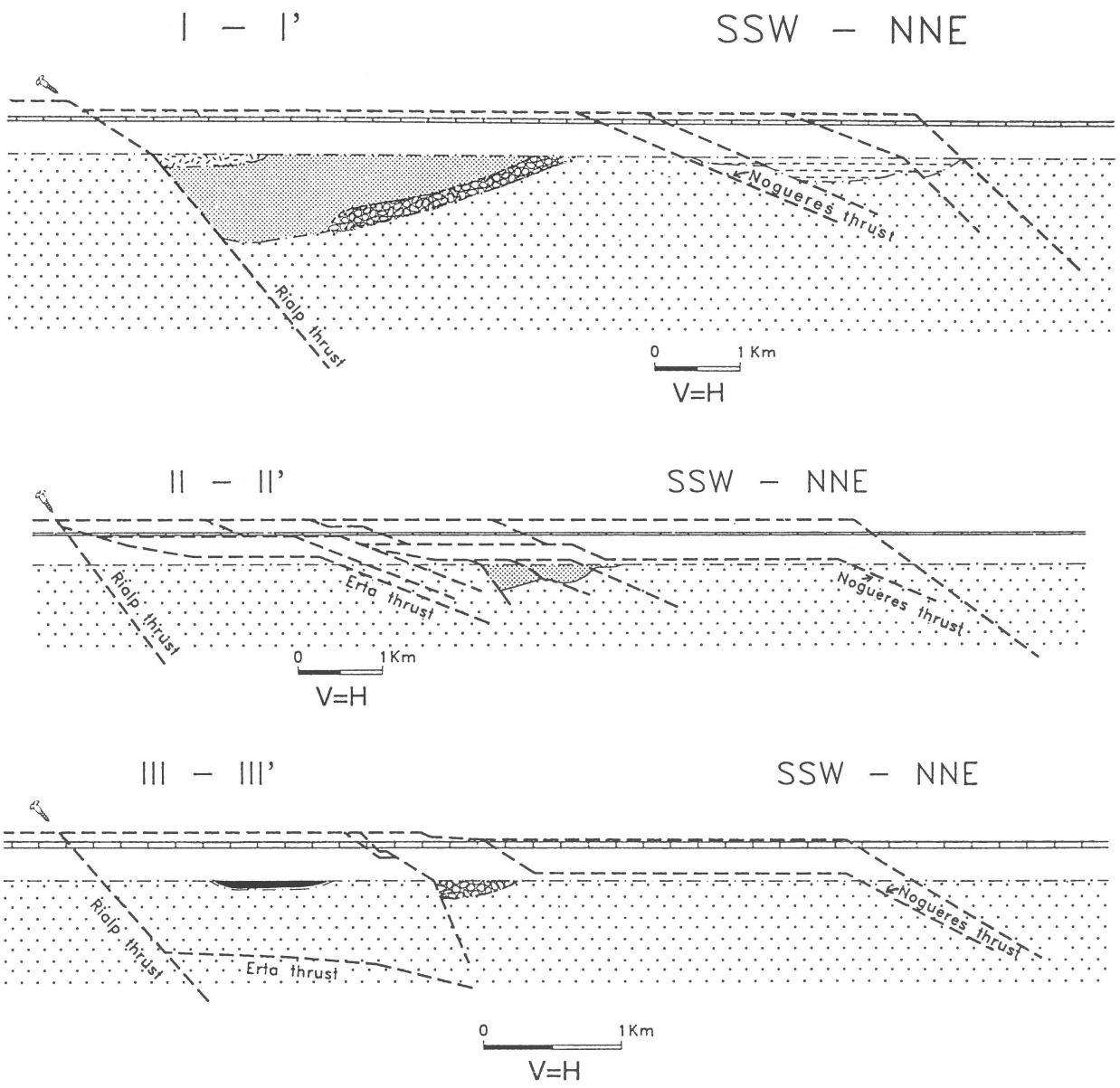

Figure 9. Restored geological cross-sections corresponding to the balanced dip cross-sections of Figure 7.

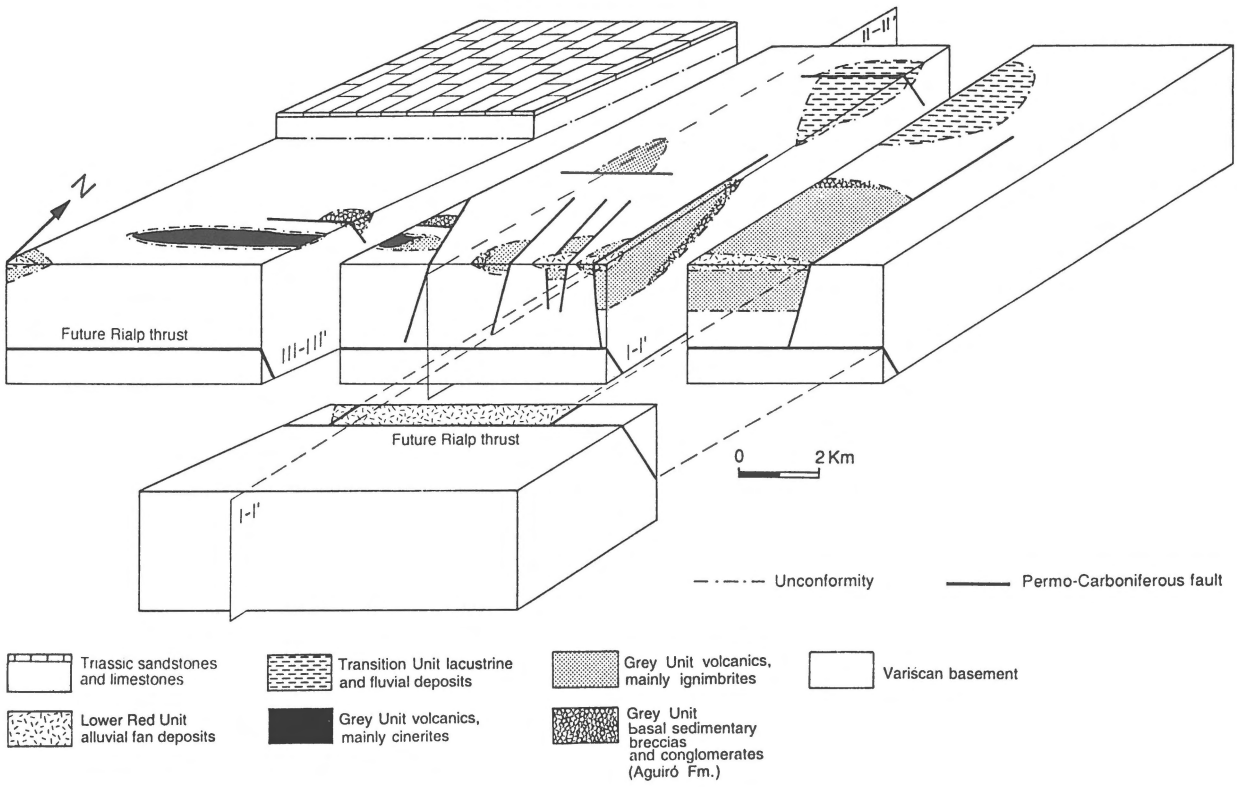

Figure 10. Reconstruction of the facies, thickness and geometry of the eastern part of the Erill Castell–Estac basin. Restored cross-sections (Figure 9) upon which reconstruction is based are also shown. The horizontal map surface corresponds to the Lower Triassic unconformity surface. Lower and Middle Triassic rocks are shown in the upper left of the diagram.

Alpine structural units involving Permo-Carboniferous rocks that are not cut by any of the sections of Figures 7 and 9 have been restored taking into account information from stratigraphic sections of the Permo-Carboniferous, and from detailed mapping of the area. Consequently, a facies distribution together with the original pre-Triassic attitude of the Permo-Carboniferous structures was obtained (Figure 10).

In the balanced sections, thrusts and Triassic and Permo-Carboniferous beds were drawn considering the structural data and the types of sedimentary or volcanic facies. The sections have been constructed using a minimum displacement hypothesis: displacements may be more than those shown in the cross-sections, but not less. Hence the N–S dimensions obtained for this part of the basin may be larger than those shown in Figure 10, but not smaller. Tentatively, 14 km in the E–W direction, and 11 km in the N–S direction are proposed as the minimum dimensions of the basin.

Restoration of cross-sections was possible since: a) the thrusting sequence and thrust transport directions are known, and the vector of regional thrust transport is in the plane of the section, b) no loss-of-volume processes have been observed in the field, and c) plane-strain may be assumed. Two key horizons were used in the restoration, a Middle Triassic limestone (brick pattern in Figures 7–9) and the Triassic unconformity. Alpine deformation along strike is negligible as deformation occurred normal to strike, so the longitudinal cross-section (Figure 8) has not been restored. Gently northward-dipping thrusts were first restored, followed by steeply southward-dipping backthrusts, and finally southward-dipping or overturned main thrusts. In the final restored cross-sections only the traces of the main thrusts are shown. The unconformity at the base of the Triassic has been chosen as horizontal datum.

The northernmost present-day exposures of Permo-Carboniferous rocks correspond to the southernmost occurrences in Figure 9, as is indicated by the results of the restoring of the geological cross-sections. This is an important feature to keep in mind in a proper reconstruction of the facies distribution. Once the sections

are restored, the Permo-Carboniferous beds are seen to form wedges that thicken to the south.

As previously stated, the Rialp thrust is the lowest outcropping thrust in this area and no Permo-Carboniferous rocks are present in its footwall. These observations allow us to interpret this thrust as a Permo-Carboniferous normal fault, which was reactivated by Alpine deformation. In a similar way, some of the E–W faults represented in Figure 10 are interpreted as originally normal faults, either totally or partially reactivated by Alpine deformation. The N–S faults also appear as normal faults, but, due to their original orientation and the orientation of the Alpine structures, they were not widely reactivated during the Alpine orogeny and, hence, controlled the thrust geometry, giving rise to lateral ramps. For example, deviations of the Erta thrust plane from its mean strike direction are interpreted to have been controlled by N–S-trending Permo-Carboniferous faults.

The palinspastic reconstruction in Figure 10 suggests the occurrence of fault blocks that produced an irregular topography (cf. Gisbert 1983; Speksnijder 1985). As an example, a major elevated zone separates the western and eastern parts of the Erill Castell–Estac basin. East of this zone, the Grey Unit and the Lower Red Unit thicken eastwards. West of the zone, both units thicken westwards.

The breccias and conglomerates at the base of the Grey Unit are interpreted as basin margin deposits (Martí 1991). In the southeastern part of the studied area, volcanic rocks reach their maximum thickness of about 1000 m. Moreover, proximal facies such as rhyolitic breccias, ignimbrites, and lavas predominate in this part, whereas thin sequences of distal volcanic rocks, 40-m-thick cinerites, are located in the west (Figure 10). Thus, the Permo-Carboniferous volcanic vents were probably located in the south, near Estac.

Discussion

The reconstruction of the Permo-Carboniferous basin, based upon detailed mapping and cross-section restoration, leads to the following observations:

1 The studied area was initially considered as part of a larger basin, named Erill Castell-Estac basin (Martí 1986, 1991). However, the facies and thickness distribution of the Grey Unit volcanics indicate that the eastern part of this basin behaved as a volcano-tectonic depression independent of the western part of the same basin. Moreover, several caldera-like episodes that took place through volcanic vents located in this eastern part produced intracaldera materials that never crop out beyond this area.

2 N–S and E–W-trending Permo-Carboniferous normal faults occur. Their age, however, is not well constrained. Facies analysis of the Estac volcanics has allowed to relate some of these N–S faults to caldera-forming collapse events, that produced Middle Stephanian intracaldera deposits. At least one N–S-trending fault is unconformably overlain by the Lower Red Unit, so it is pre-Early Permian (Figure 10). Other N–S faults may be synchronous with the deposition of the Middle Stephanian–Early Permian series in the studied area, but they might also postdate this series and be Late Permian faults, developed prior to the deposition of the Lower Triassic. The significant erosion that took place between the end of the Variscan orogeny and the onset of the Lower Triassic sedimentation precludes their age to be better constrained.

Conclusions

The approach followed in this study has allowed us: 1) to constrain the minimum basin dimensions for the studied part of the Erill Castell–Estac basin, 2) to establish the paleogeographic position of Permo-Carboniferous rocks, 3) to differentiate the eastern part of the basin as a volcano-tectonic depression independent of the western part, 4) to recognize E–W and N–S-trending Permo-Carboniferous normal faults, some of them not described before, and 5) to gain insight into the probable age of N–S-trending Permo-Carboniferous faults.

Finally, we believe that the type of study reported here permits a complete view of the evolution of the Permo-Carboniferous series and could be extended to other basins, in order to achieve a regional overview of Permo-Carboniferous basins throughout the Pyrenees.

Acknowledgements

This paper was supported financially by the Dirección General de Investigación Científica Tecnologia (DGICYT) project PB91-0252, and by the Comissionat per Universitats i Recerca de la Generalitat de Catalunya, Grup de qualitat GRQ94-1048. J.M. is grateful for a European Commission contract (ERBCH-

BICT93052) of the Human Capital and Mobility Programme. Detailed comments by S. Johnson have greatly improved an earlier version of the manuscript and are gratefully acknowledged. We also thank A. Speksnijder for careful reviews that enabled us to improve substantially this contribution.

References

Alvarez-Ramis, C. 1985 Sobre la presencia de flora Autuniense en las series carboníferas del pirineo leridano (España). X Congr. Intern. Strat. y Geol. Carbonifère, Madrid 2: 181–189

Besly, B.M. & J.D. Collinson 1991 Volcanic and tectonic controls of lacustrine and alluvial sedimentation in the Stephanian coal-bearing sequence of the Malpas-Sort Basin, Catalonian Pyrenees – Sedimentology 38: 3–26

Bixel, F. & C. Lucas 1983 Magmatisme tectonique et sédimentation dans les fosses stéphano-permiens des Pyrénées occidentales – Revue Géogr. Phys. Géol. Dynam. 24: 329–342

Broutin, J. & J. Gisbert 1985 Entorno paleoclimático y ambiental de la flora del Stephano-Autuniense del Pirineo Catalán. X Congr. Intern. Strat. Geol. Carbonifère Madrid 3: 53–66

Dalloni, M. 1910 Etude géologique des Pyrénées de l'Aragon – Ann. Fac. Sci. Marseille 19: 1–444

Gilbert, J.S. 1989 The Late-Hercynian volcanism of the Pyrenees (unpublished PhD thesis). Cambridge University, Cambridge, 325 pp

Gilbert, J.S. & N.W. Rogers 1989 The significance of garnet in the Permo-Carboniferous volcanic rocks of the Pyrenees – J. Geol. Soc. London 146: 477–490

Gisbert, J. 1981 Estudio geológico-petrológico del Estefaniense-Pérmico de la Sierra del Cadí (Pirineo de Lérida). Diagénesis i sedimentología (unpublished PhD thesis). Zaragoza University, Zaragoza, 313 pp

Gisbert, J. 1983 El Pérmico de los Pirineos españoles. In: J. Martínez-Diaz (ed.) Carbonífero y Permico de España II – Inst. Geol. Min. Esp. Madrid: 405–420

Hartevelt, J.J.A. 1970 Geology of the upper Segre and Valira valleys, Central Pyrenees, Andorra/Spain – Leidse Geol. Meded. 45: 349–354

Hess, J.C. & H.T. Lippolt 1986 $^{40}Ar/^{39}Ar$ ages of tonstein and tuff sanidines: new calibration points for the improvement of the Upper Carboniferous time scale – Chemical Geology (Isotope Geosciences section) 59: 143–154

Martí, J. 1986 El vulcanisme explosiu Tardihercinià del Pirineu Català (unpublished PhD thesis). Barcelona University, Barcelona, 303 pp

Martí, J. 1991 Caldera-like structures related to Permo-Carboniferous volcanism of the Catalan Pyrenees (NE Spain) – J. Volcanol. Geothermal Res. 45: 173–186

Martí, J. & J. Mitjavila 1988 El volcanismo tardihercínico del Pirineo Catalán, II: Caracterización de la actividad explosiva – Acta Geol. Hispan. 23: 21–31

Mey, P.H.W., P.J.C. Nagtegaal, K.J. Roberti & J.J.A. Hartevelt 1968 Lithostratigraphic subdivision of post-Hercynian deposits in the south-central Pyrenees, Spain – Leidse Geol. Meded. 41: 221–228

Muñoz, J.A. 1992 Evolution of a Continental Collision Belt: ECORS–Pyrenees Crustal Balanced Cross-section. In: K. McClay (ed.): Thrust tectonics, Unwin & Hyman, London: 235–246

Nagtegaal, P.J.C. 1969 Sedimentology, paleoclimatology and diagenesis of post-Hercynian continental deposits in the South-Central Pyrenees – Leidse Geol. Meded. 42: 143–238

Poblet, J. 1991 Estructura de les unitats del vessant sud de la zona axial del Pirineu central (unpublished PhD thesis). Barcelona University, Barcelona, 604 pp

Self, S. 1983 Large-scale phreatomagmatic silicic volcanism: a case study from New Zealand – J. Volcanol. Geothermal Res. 17: 433–469

Self, S., F. Goff, J.N. Gardner, J.V. Wright & W.M. Kite 1986 Explosive rhyolitic volcanism in the Jemez mountains: Vent location, caldera development and relation to regional structure – J. Geophys. Res. 91: 1779–1798

Soula, J.-C., C. Lucas & G. Bessiere 1979 Genesis and evolution of Permian and Triassic basins by regional simple shear acting on older Variscan structures: field evidence and experimental models – Tectonophysics 58: T1–T9

Speksnijder, A. 1985 Anatomy of a strike-slip controlled sedimentary basin, Permian of the Southern Pyrenees, Spain – Sedimentary Geol. 44: 179–223